Supporting Information

Light-Initiated Aggregation of Gold Nanoparticles for Synergistic Chemo-Photothermal Tumor Therapy

Huawei Xia [a,#], Jinfeng Zhu [a b,#], Changhe Men [a], Anna Wang [a], Qiulian Mao [a], Yali Feng [a], Jiachen Li [a], Jingwei Xu [c], Xiaju Cheng [a,], Haibin Shi [a,*]*

[a] State Key Laboratory of Radiation Medicine and Protection, School for Radiological and interdisciplinary Sciences (RAD-X) and Collaborative Innovation Centre of Radiation Medicine of Jiangsu Higher Education Institutions, Soochow University, 199 Renai Road, Suzhou 215123, China.

[b] Department of Experimental Medicine, TOR, University of Rome Tor Vergata, 00133 Roma, Italy.

[c] Department of Cardiothoralic Surgery, Suzhou Municipal Hospital Institution, Suzhou 215002, P. R. China.

[#]Equal contribution authors.

[*]Co-corresponding author: XJ Cheng (xjcheng@suda.edu.cn), HB Shi (hbshi@suda.edu.cn)

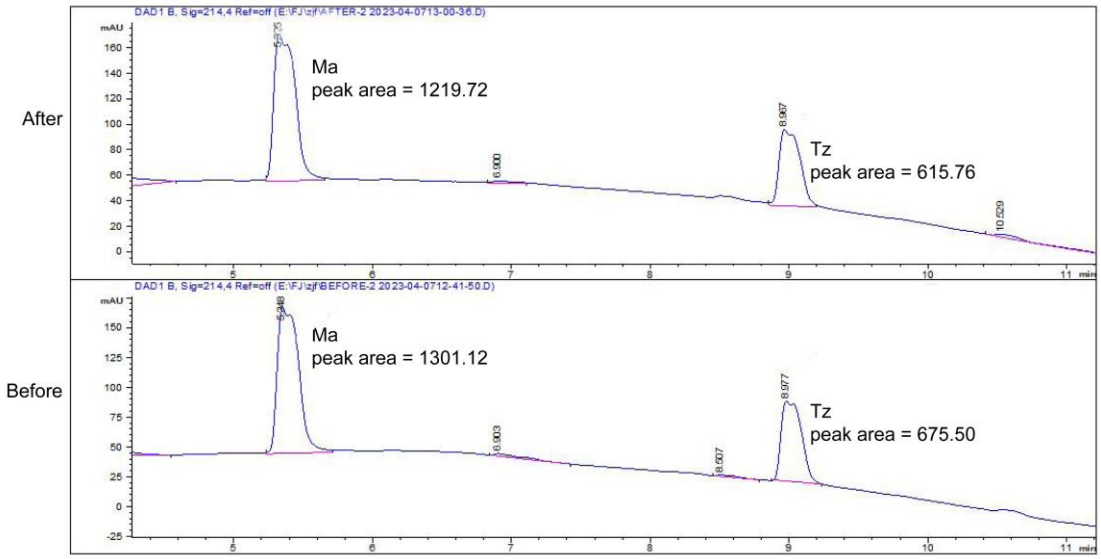

Figure S1. The loading content of Tz and Ma were detected by HPLC before and after reaction with Au-PEG-NH_2.

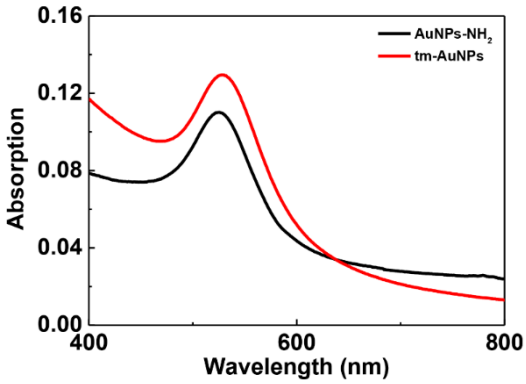

Figure S2. The absorption spectra of the AuNP-NH_2 and the tm-AuNPs.

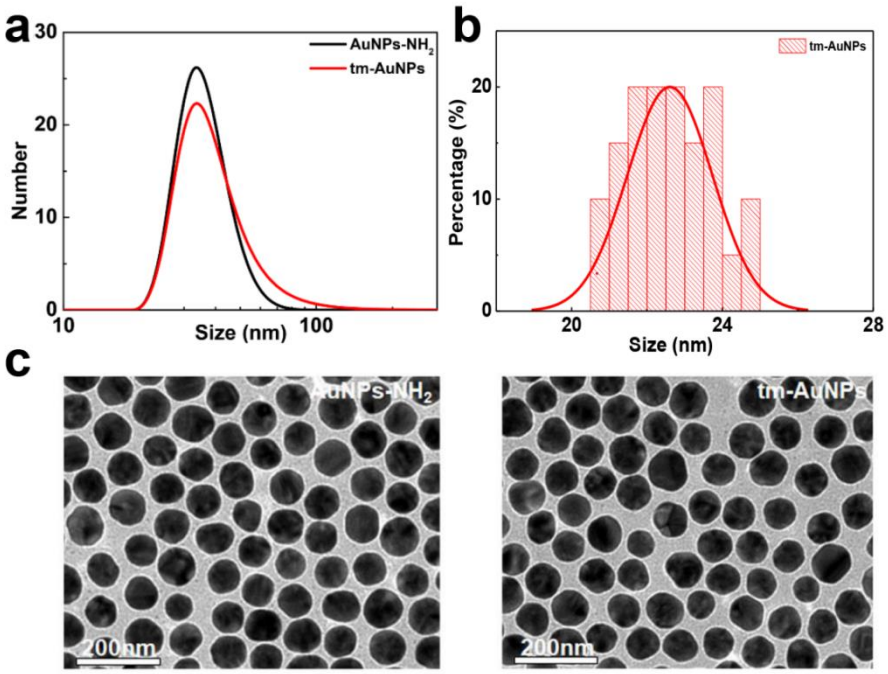

Figure S3. (a). the hydrodynamic size of the AuNPs-NH_2 and the tm-AuNPs, (b). statistical histogram of the size distribution of tm-AuNPs, counted from 120 nanocrystals shown in typical TEM images, (c). Transmission electron microscopy (TEM) images of the AuNPs-NH_2 and the tm-AuNPs.

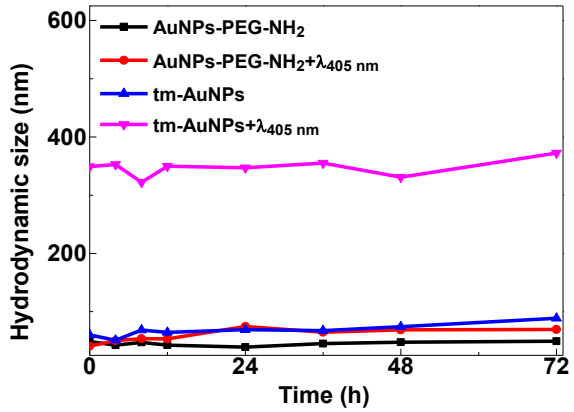

Figure S4. Temporal evolution of hydrodynamic size of AuNPs-NH_2 and tm-AuNPs treated with 405 nm irradiation for comparing with those receiving no laser treatment. (405 nm:1 W/cm^2, t = 25 min).

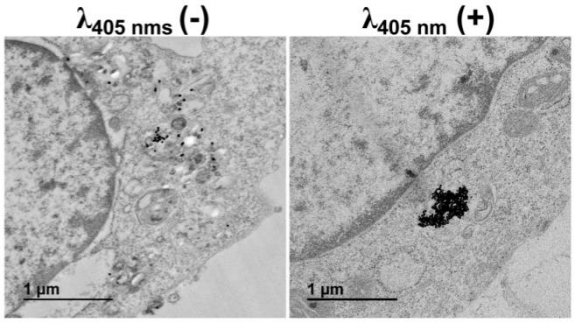

Figure S5. TEM images for showing the light-initiated crosslinking behavior of tm-AuNPs in living cells.

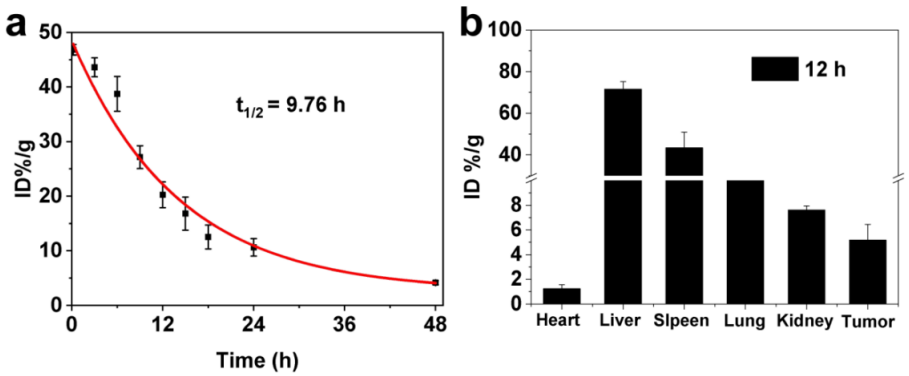

Figure S6. (a) The blood circulation behavior of tm-AuNPs, (b) The biodistribution of tm-AuNPs in various organs and tumor of the tumor-bearing mice at 12 h post-injection.

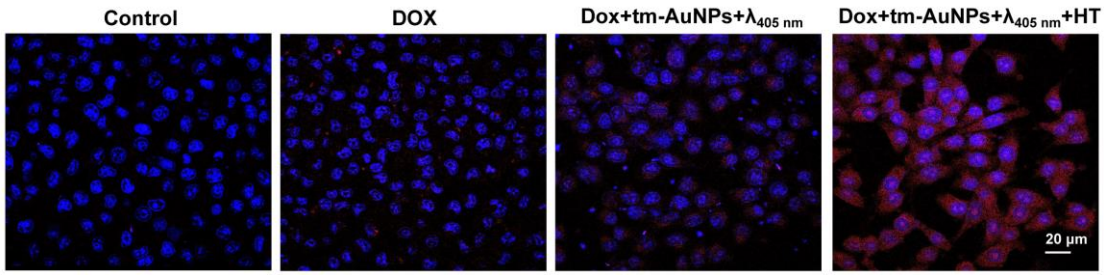

Figure S7. Fluorescence images for showing the cellular uptake of DOX in tumor cells.

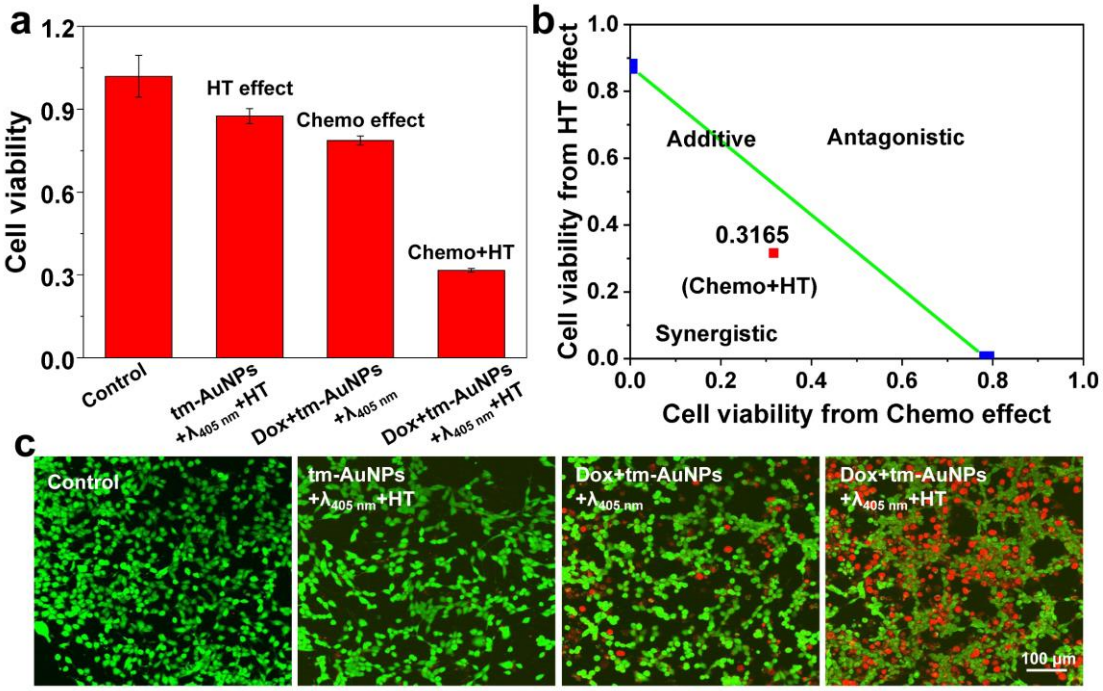

Figure S8. (a) Cell viability characterization of 4T1 cells with different treatments, (b) Isobologram analysis of the synergistic anticancer effect of the combined hyperthermia and chemotherapy in 4T1 cells. The data points in isobologram corresponding to the growth inhibition ratio in the combination treatment, (c) The live/dead staining of 4T1 cells with different treatments.

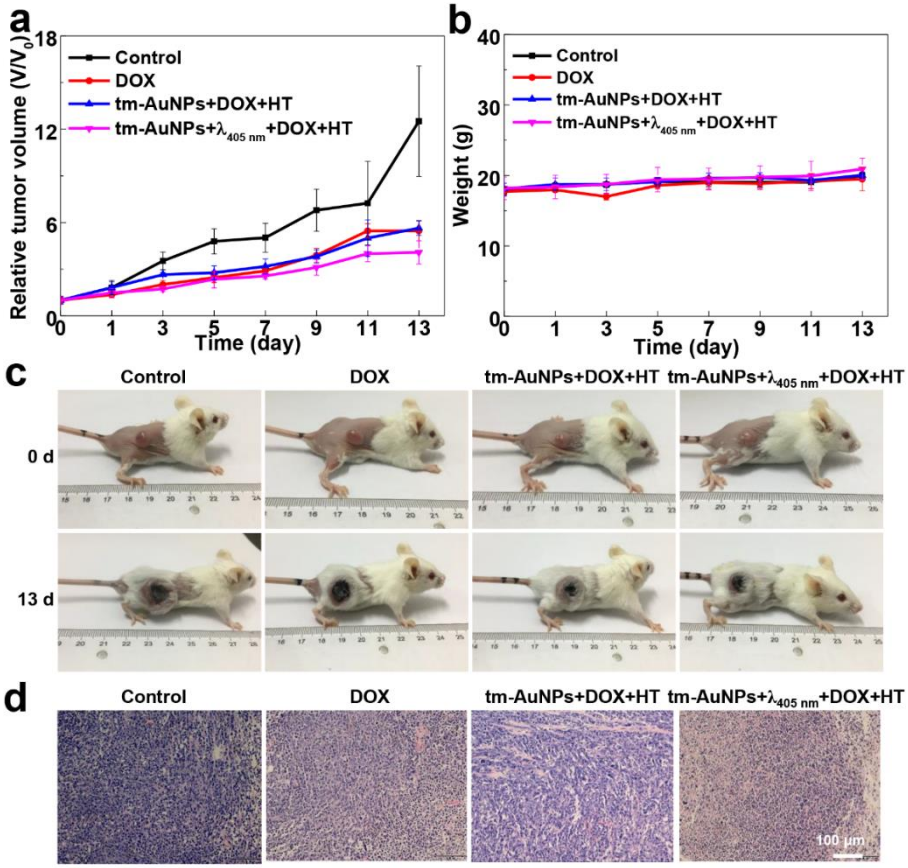

Figure S9. (a) tumor volume and (b) mice body weight of taking different combination treatments (n = 4), (c) Photographs of representative mice chosen from each group, (d) H&E staining of Tumor tissue on 3rd day post-treatment for viewing the therapeutic efficacy of different combination treatments.

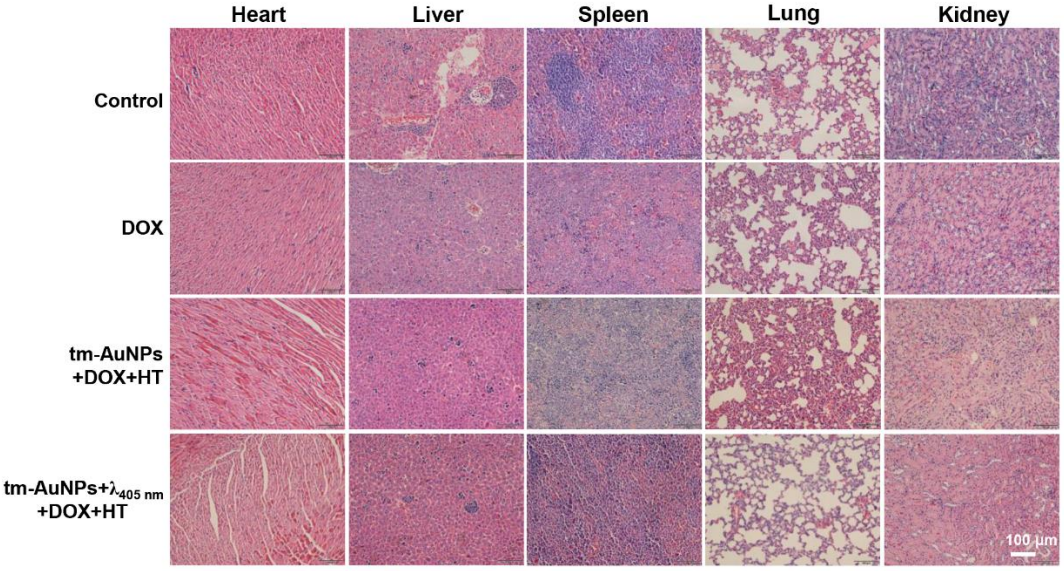

Figure S10. Representative H&E staining pictures of heart, liver, spleen, lung, and kidney of tumor-bearing mice on last day post-treatment.

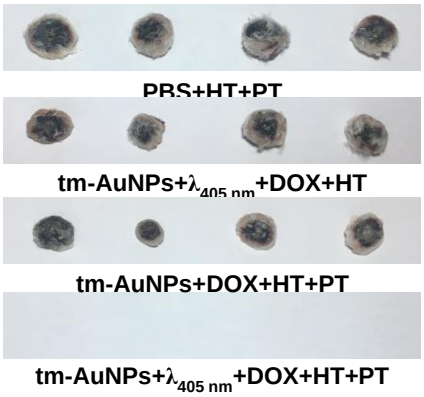

Figure S11. Photographs of tumors harvested on the last day post-treatments from mice receiving different treatments.

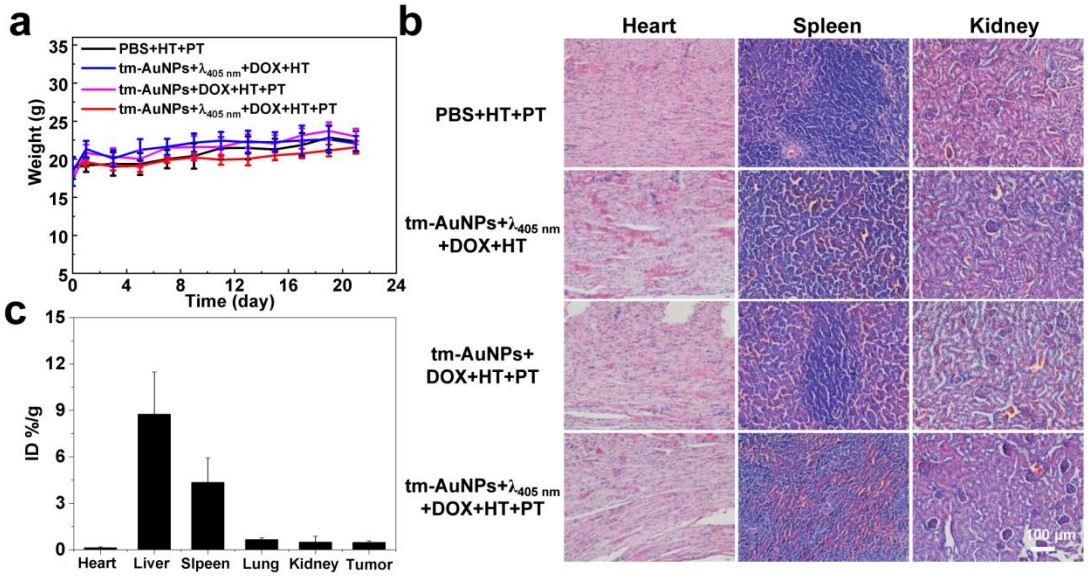

Figure S12. (a) Mice body weight of taking different combination treatments (n = 4), (b) Representative H&E staining pictures of heart, spleen, and kidney of tumor-bearing mice on last day post-treatment, (c) the Au content in various organs and tumor of the tumor-bearing mice on last day post-treatment.